



Validating a Novel Theoretical Expression for Burn time and Average Thrust in Solid Rocket Motor Design

B. K. Aliyu^{1*}, C. A. Osheku¹, E. O. Oyedeji¹, M. A. L. Adetoro¹, A. A. Okon¹
and C. M. Idoko¹

¹Federal Ministry of Science and Technology (FMST), National Space Research and Development Agency (NASRDA) Centre for Space Transport and Propulsion (CSTP), Epe-Lagos Nigeria.

Authors' contributions

This work was carried out in collaboration between all authors. Author CAO formulated the novel burn time expression. Author BKA designed the study, extended the novel expression to include average thrust and Specific impulse, introduced the concept of importing DAQ results into MATLAB for analysis and wrote the first draft of the manuscript. Author MALA managed the experimental process.

Author AAO computed the experimental values of burn time, average thrust, and specific impulse also, he plotted all SRM profiles in MATLAB. Author CMI designed and prepared the solid rocket fuel Sorbitol. Author EOO ensured the chamber design, managed literature searches, and analysis of the study. All authors read and approved the final manuscript.

Article Information

DOI: 10.9734/AIR/2015/18468

Editor(s):

- (1) Martin Kröger, Professor Computational Polymer Physics Swiss Federal Institute of Technology (ETH Zürich), Switzerland.
- (2) José Alberto Duarte Moller, Center for Advanced Materials Research, Complejo Industrial Chihuahua, Mexico.
- (3) Francisco Marquez-Linares, Full Professor of Chemistry, Nanomaterials Research Group, School of Science and Technology, University of Turabo, USA.

Reviewers:

- (1) Yordanka Tasheva, "Industrial Technologies and Management", Bulgaria.
- (2) Anonymous, Ming Chi University of Technology, Taiwan.
- (3) Anonymous, India.

Complete Peer review History: <http://sciencedomain.org/review-history/10187>

Original Research Article

Received 23rd April 2015
Accepted 1st July 2015
Published 15th July 2015

ABSTRACT

A major application of solid propellants is in gun propulsion systems and rockets. The performance of a rocket depends greatly on the design of the solid propellant that meets a specific mission. Performance characteristics such as the burn time, burn rate, average thrust, specific impulse, characteristic velocity, etc., are basic design parameters that will determine the nature of the

*Corresponding author: E-mail: aliyu_bhar@yahoo.com;

trajectory and maximum altitude attained by such rocket. The main objective of this study, is to derive a novel analytical expression for *burn time* and average thrust as a function of grain length and web thickness and compare experimental results from a static test bed with that of the analytical formulation. Here, a Sugar propellant (SP), *sorbitol* ($C_6H_{14}O_6$) consisting of an oxidizer, potassium nitrate (KNO_3), is locally propounded. In this study, five Solid Rocket motors (SRM) are under investigation, *bate* grain geometry were implemented and were subjected to a static thrust test. Data from the static thrust tests were acquired via a Digital Acquisition System (DAQ) and imported into MATLAB environment for the time verse thrust profile plot and other computations. The mathematically derived formulations for the burn time and average thrust gave a good correlation with experimental values for all the SRMs, with errors of less than 10 per cent.

Keywords: Solid rocket motor; sorbitol; static thrust test; burn time; average thrust.

1. INTRODUCTION

In solid-propellant rocket motors, the propellant to be ignited is contained within the combustion chamber or motor case. The motor case is effectively a pressure vessel that is designed to contain the high gas pressures required for propellant combustion which for black-powder propellant is in the range of 0.69 MPa to 6.9 MPa [1]. The solid propellant charge is called the grain and it contains all the chemical elements for complete burning (i.e. oxidizer, fuel). Once ignited by the ignition system (which is usually an electrical fuse), the grain usually burns smoothly at a predetermined rate on all exposed surfaces of the grain. The exposed grain surfaces continue to recede during burning in a combination of tangential and perpendicular directions to the exposed surfaces until the propellant is totally consumed. The resulting hot gas flows through the convergent-divergent nozzle to produce thrust. For most solid-propellant motors, once they are ignited they cannot be extinguished and the thrust cannot be randomly throttled in any way. Almost all solid-propellant rocket motors are used only once. The hardware that remains after all the propellant has been burned and the mission completed—namely the motor (nozzle, bulkhead and chamber)—is not reusable [2]. Fig. 1 below shows the cross sectional diagram of the SRM designed at Centre for Space Transport and Propulsion (CSTP). Each motor will contain the propounded propellant and will be tested before assembling it into a rocket structure.

The motor grain is the solid body of the hardened propellant and typically accounts for 82% to 94% of the total motor mass. Grains can have many geometry type including slots, grooves, holes, or even no cavities at all which are known as end-burning grains. The various types of grain

geometries and their associated thrust-time profiles as presented in Fig. 2 [3].

The shape of the thrust-time profile depicted in Fig. 2 depends on how the grain exposed surface area changes over the motor's burn time. The various grain geometries alter the initial burning surface, which determines the initial mass flow rate and the initial thrust. The hot reaction gases of the burnt propellant flow along the perforation or grain cavity toward the nozzle. For amateur model rockets where maximum achievable altitude is desired, a high boost thrust is desired to apply initial acceleration, but, as propellant is expended and the vehicle weight is reduced, a decrease in thrust is desirable; this often reduces the drag losses, and usually permits a more effective flight path. Therefore, there is a benefit to vehicle mass, flight performance, and cost in having a higher initial thrust during the *boost phase* of the flight, followed by a lower thrust (often 10% to 30% of the boost thrust) during the *sustained phase* of the powered flight, typical SRMs with such trends are of Estes C6-0, D11-P and D12-0 SRMs [4] which can be depicted schematically as shown in Fig. 3.

Solid propellants could either be a SP or ammonium perchlorate (AP) based. SPs have been used by rocket hobbyist since the 1940's. These propellants consist of an oxidizer, combined with a sugar. At least four methods have been used to prepare sugar propellants these are, dry ramming, melting and casting, moist pressing, and recrystallization. A lot of research has been done on SPs in the past hence, they are now well-characterized and predictable. The specific impulse (I_{sp}) of SPs are not as high as many AP based propellants, though SPs have the advantage of being simple to prepare and require very simple equipment [5]. SPs are moderate-performance propellants in

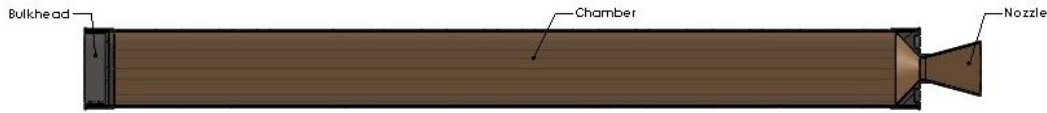


Fig. 1. Cross-section of the SRM.

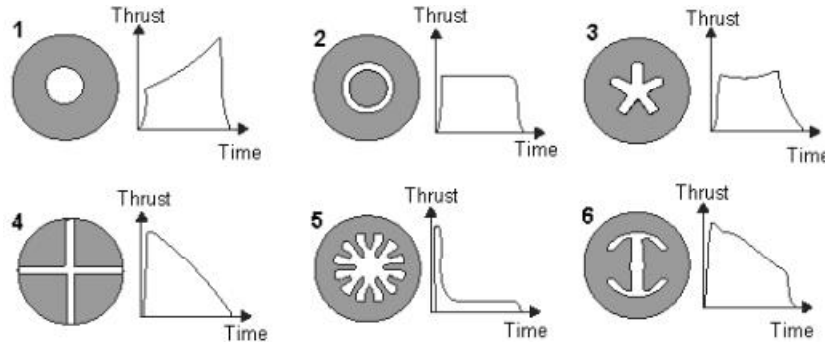


Fig. 2. Various typical propellant grain cross-sections and associated thrust-time profiles

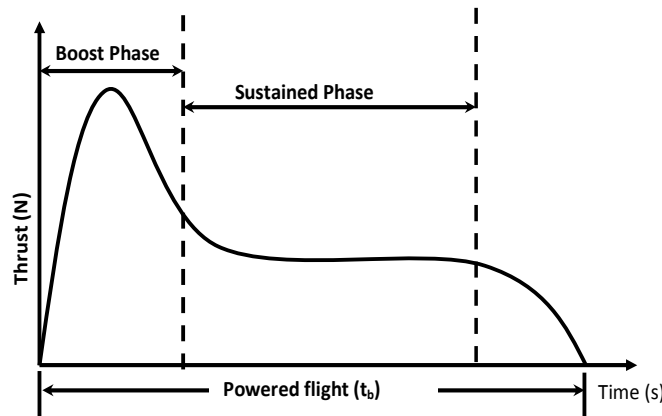


Fig. 3. Boost and sustained phases of a typical armature SRM

which the binder-fuel is one of the common sugars (sucrose, dextrose, maltose, etc.). They are designated KN for potassium nitrate as the oxidizer. Some of such SPs are; KNSB for sorbitol fuel, KNDX for dextrose fuel, and KNSU for sucrose fuel.

William Colburn of the Rocket Missile Research Society carried out the first experiments with KN/sucrose in 1944 and the first sugar based propellant rocket launch was in 1944. Bill Colburn via Richard Nakka's website mentioned that the first propellant, designated TF-1 was by dry-mixed KN/sucrose moistened with water and pressed into the motor tube. Woody Stanford of Stanford Systems and Jon Drayna of October Science each by 2002 had already began producing and marketing kits for making sugar-propelled rocket engines.

2. Solid Propellant Chemistry

This section will first discuss the general chemical properties of solid propellant, and then secondly, focus will be on KNSB used for the five SRMs in this study.

The combustion behaviour of a solid propellant is generally characterized by the steady linear regression rate of the burning surface known as the burning rate (r_b) and is regarded as one of the most important performance parameters. It is expressed as:

$$r_b = f(P, T_0, O_p, \phi, C-F, U_g, G_p), \quad (1)$$

where, P is the pressure; T_0 , the initial grain temperature; O_p the oxidizer particle size; ϕ , the oxidizer-fuel mixture ratio; $C-F$, the chemical

formulation of the propellant; Ug , the transverse velocity of the combustion gases wetting the burning surface and Gp , the propellant grain shape factor. One of the most widely used techniques to determine r_b is the closed bomb technique [6]. In this method, pressure variation with time is measured. The pressure is allowed to build up, thereby accelerating combustion. The pressure is recorded as a function of time. At any time, t , the value of r_b is then determined by the instantaneous pressure prevailing therein at that instant. Hence, r_b is calculated using the following empirical relationship [7]:

$$\ln\left(\frac{dP}{dt}\right) = \ln\left(\frac{qa_1}{LC_pT_0}\right) + (1+n)\ln P, \quad (2)$$

Where, L is the length of the cylindrical sample; q , the heat of combustion in cal / g; n , the number of moles of the gas; and a_1 is a constant. Thus, a plot of $\ln(dP/dt)$ vs $\ln P$ will give a straight line with a slope of $(1+n)$ and intercept of $\ln(qa_1/LC_pT_0)$, where C_p is the specific heat. From the intercept, a_1 could be calculated, since other parameters, q , L , C_p and T_0 are known. Hence, the value of r_b is computed at a desired pressure.

After experimenting with six different motors (varying web thickness and grain length) made with sorbitol as the propellant, we arrived at the results in Table 1.

A graphical representation of motor length against burn time for Table 1 gave the result in Fig. 4. This was interpreted as a decreasing trend: As motor length increases burn time decreases.

We desire to validate the trend in Fig. 4 with a theoretical expression, this quest lead us to interesting information in *ATK Space Propulsion Catalogue* [8]. We extracted some SRMs from the catalogue and tabulated them in Table 2 and the graphical representation plotted in Fig. 5

We interpreted Fig. 5 to have the same trend as that of Fig. 4 -increase in motor length L results in decrease in burn time, t_b . Hence, we are urged that the motor length L plays a significant role in the value of the burn time, which inversely related to the burn rate, r_b . The notion that r_b as a function of only web thickness w is old and quite popular, dating as far back as the work Miller and Barington in 1970 [9]. A lot of recent research has been done relating burn rate with both the length L and web thickness w of the propellant grains [10,11,12].

In this study, we are keenly interested in t_b as it relates to w and L . Burn time of an SRM during static test translates to a rocket's time of powered flight (from take-off up to propellant burnout) [13]. Hence, burn time could be used to analyse the trajectory of the entire rocket to accurately ascertain the maximum altitude a rocket will attain during trajectory design and simulation.

2.1 Sorbitol

Sorbitol is a six carbon polyalcohol characterized by extensive hydrogen bonding. It provides excellent working time in melted form and provides a slightly longer t_b than Sucrose SRMs. Sorbitol has the following synonyms; D-Glucitol, D-Sorbitol, and Sorbitol. It is very soluble in water and slightly soluble in ethanol, and its chemical structure is depicted in Fig. 6.

Table 1. Experiment for burn rate

| S/N | w(m) | L(m) | t_b (s) | \dot{r}_b (m/s) |
|-----|-------|-------|-----------|-------------------|
| 1 | 0.034 | 0.175 | 8.6 | 0.024 |
| 2 | 0.028 | 0.285 | 4.5 | 0.070 |
| 3 | 0.034 | 0.350 | 5.3 | 0.070 |
| 4 | 0.034 | 0.525 | 7.3 | 0.080 |
| 5 | 0.028 | 0.285 | 3.6 | 0.090 |
| 6 | 0.034 | 0.525 | 6.7 | 0.080 |

Table 2. Three SRMs from ATK catalogue

| S/N | SRM | D(m) | L(m) | t_b (s) |
|-----|-------------|------|------|-----------|
| 1 | ORION 50S | 1.27 | 8.7 | 75.3 |
| 2 | ORION 50SXL | 1.27 | 10.3 | 69.1 |
| 3 | ORION 50XLT | 1.27 | 9.8 | 68.4 |

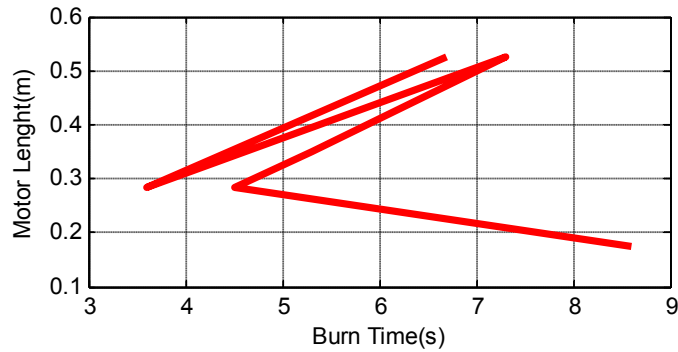


Fig. 4. Graph of Burn time against motor length

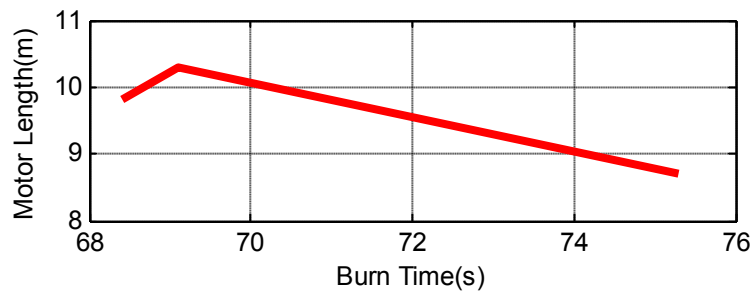
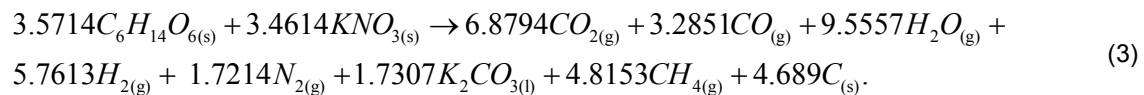


Fig. 5. ATK Catalogue SRMs burn time against motor length

For the KNSB propellant, with 65 per cent Sorbitol and 35 per cent Potassium nitrate, the theoretical combustion equation in (3) was realised using the software ProPEP (*Propellant Performance Evaluation Program*) at a pressure of 1000psi (6.8 MPa),



While there are many different grain designs that can be utilized in motor design, the bate grain is probably the most common and the simplest. For this study, the propellant for the five SRMs is sorbitol based with a bate grain as shown in Fig. 7; A burn inhibitor was wrapped around the grains to ensure uniform burning from the core to the outer wall. The inhibitor was glued to the propellant with epoxy to prevent delamination.

Where, w is the grain web thickness, and l is the bate length. The motor dimensions (case outer diameter D , and cylindrical motor length, L). All 5 SRM in this study have, $D = 0.105m$, $d=0.05m$, $l=0.172 m$, $L=0.52 m$, $w=0.0275 m$, with number of bate as, $N=3$ and density of $1.837 [gc/m^3]$. Due to preparation lapses, motor masses differ; SRM 1 has a mass of $5.87 kg$, SRM 2 is $6.18 kg$, SRM 3 and SRM 4 have the same mass of $6.27 kg$,

and SRM 5 is $6.1774 kg$. All masses could be approximated to $6 kg$

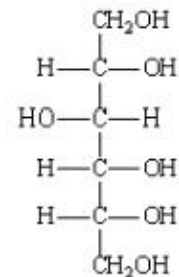


Fig. 6. Chemical structure of Sorbitol

2.2 Design Objective

The goal of sounding rockets is to attain higher altitude at the cheapest cost possible without

compromising safety at any level of the design. The property of sorbitol based SRM to have a longer burn time than sucrose based motor is the main property of attraction. Longer burn time (especially at the sustained phase of the thrust, see Fig. 3), coupled with a reasonably high average thrust means a longer powered flight of the rocket. This will surely translate to a longer coasting phase and as a whole, higher altitude will be attained by the rocket. In this study, we choose to put forward a novel theoretical expression that will predict burn time and average thrust as a function of propellant web thickness, and length of cylindrical motor, amongst other variables.

3. Derivation for Burn time and Maximum Thrust

In this section, an analytic approach will be employed based on pre-existing designed grain geometry developed at CSTP to formulate a closed-form formula for burn time and maximum thrust for the sorbitol based solid rocket propellant.

Considering a cylindrical bate geometry for the propellant as show in Fig. 8, with a motor length L , web thickness w , with inner and outer diameters of d and D .

We assume that when burning is initiated at one end, the resultant direction in which combustion flames progresses are, tangentially along the length of the motor L and perpendicularly across the web thickness w as shown in Fig. 8. Taking burn rate as, $r_b = 0.0688\text{m/s}$ (average from Table 1), we propose that burn time be expressed differently as

$$t_b = \frac{w+L}{r_b}. \quad (4)$$

Aspect ratio is given as

$$L = D\eta. \quad (5)$$

The radius of the circular face of the hollow cylinder can be expressed in terms of the inner diameter as given in (6) and the web thickness as in (7) respectively.

$$d = 2r \quad (6)$$

$$w = \frac{D-d}{2} \quad (7)$$

From (7), we can write

$$D = 2w + d \quad (8)$$

Substituting (5) in (4), we get

$$t_b = \frac{w + D\eta}{r_b} \quad (9)$$

Now substituting (8) in (9), expanding the numerator and collecting like terms will yield

$$t_b = \frac{w(1+2\eta) + d\eta}{r_b}. \quad (10)$$

Hence, from (10), we can conclusively say that the burn time is a function of both the web thickness w and the length of the cylindrical grain L (a function of the aspect ratio). Thus, we proceed to derive a formula for the thrust.

Area of the bate disk is given by

$$A = \frac{\pi(D^2 - d^2)}{4}. \quad (11)$$

Substituting (8) in (11) gives,

$$A = \pi(w^2 + wd). \quad (12)$$

The volume of the grain is deduced as

$$V = \pi L(w^2 + wd). \quad (13)$$

Mass of the propellant is given as

$$m_p = \pi L(w^2 + wd)\rho_p. \quad (14)$$

Expression for the average thrust (given specific impulse, gravity and density values) will be

$$F_{avg} = \frac{1}{t_2 - t_1} [s^{-1}] \int_{t_1}^{t_2} F dt [N.s] = \frac{m_p I_{sp} g}{t_b} [N], \quad (15)$$

Substituting (10) and (14) in (15) we arrived at an expression for average thrust as a function of web thickness and propellant grain as;

$$F_{avg} = \frac{\pi L(w^2 + wd)r_b \rho_p I_{sp} g}{w(1 + 2\eta) + d\eta} \left[\frac{m.kg}{s^2} \right]. \quad (16)$$

Mathematically, Total impulse I_T is the thrust force integrated over the burn time given as

$$I_T = \int_{t_1}^{t_2} F dt [N.s], \quad (17)$$

The specific impulse is defined as the total impulse per unit weight of propellant burned hence, we can go ahead and write this expression as:

$$I_{sp} = \frac{I_T [N.s]}{g m_p [N]} = \frac{F_{avg} \{w(1 + 2\eta) + d\eta\}}{\pi L(w^2 + wd)r_b \rho_p g}. \quad (18)$$

4. EXPERIMENTAL SETUP

A thrust-measuring system usually requires one or more sensing elements (transducers). Recording of rocket test data has been performed in several ways, such as on magnetic tapes, disks and by computers. The *range* of a thrust measuring system is usually limited by instrument yield strength and/or the *linear operating range*. The linear operating range implies that the system will become increasingly

nonlinear beyond the maximum and minimum limits. Usually an additional margin is provided to permit temporary overloads without damage to the system or need for recalibration and to ensure measurements lie in the system linear range [14].

In this study, the measuring instrument basically comprises of a load-cell with a maximum measurable load of 5kN and a computer for recording as depicted in Fig. 9.

To obtain useful data from the load-cell transducer, a data DAQ system was required as well as an electrical power supply and electronic amplifier/signal conditioner. The DAQ system used for this experiment was developed by *DATAQ Instruments*. This DAQ system consisted of a software suite which was installed on a laptop computer, a channel-conditioning bus board and the necessary electrical cables. The electrical power supply and electronic amplifier/signal conditioner were contained in one unit. To get meaningful thrust-time profiles of the motors, the mass of the motor case and propellant were taken separately and when the propellant was loaded in the combustion chamber, it was also measured before placing them on the load cell. These masses had to be subtracted from the measured thrust values.

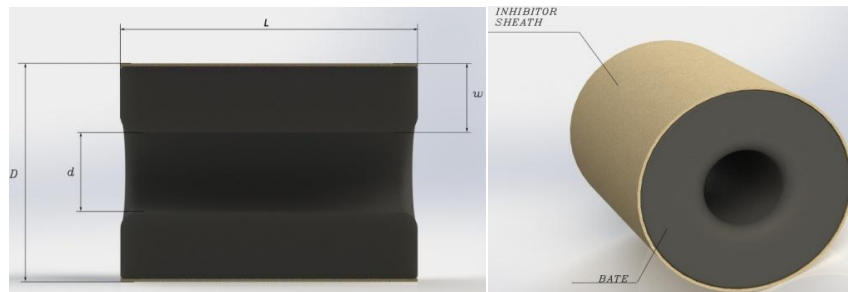


Fig. 7. Cylindrical baffle geometry for a SRM

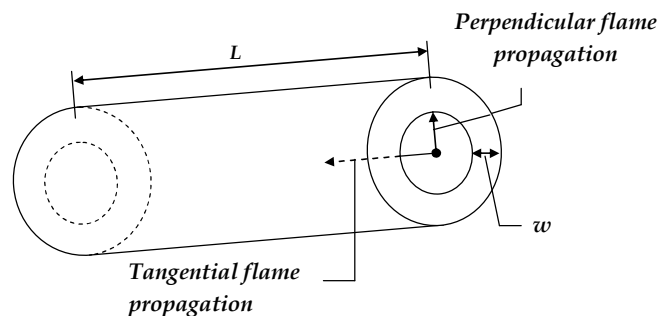


Fig. 8. Flame propagation during combustion in a cylindrical SRM with end-burn.

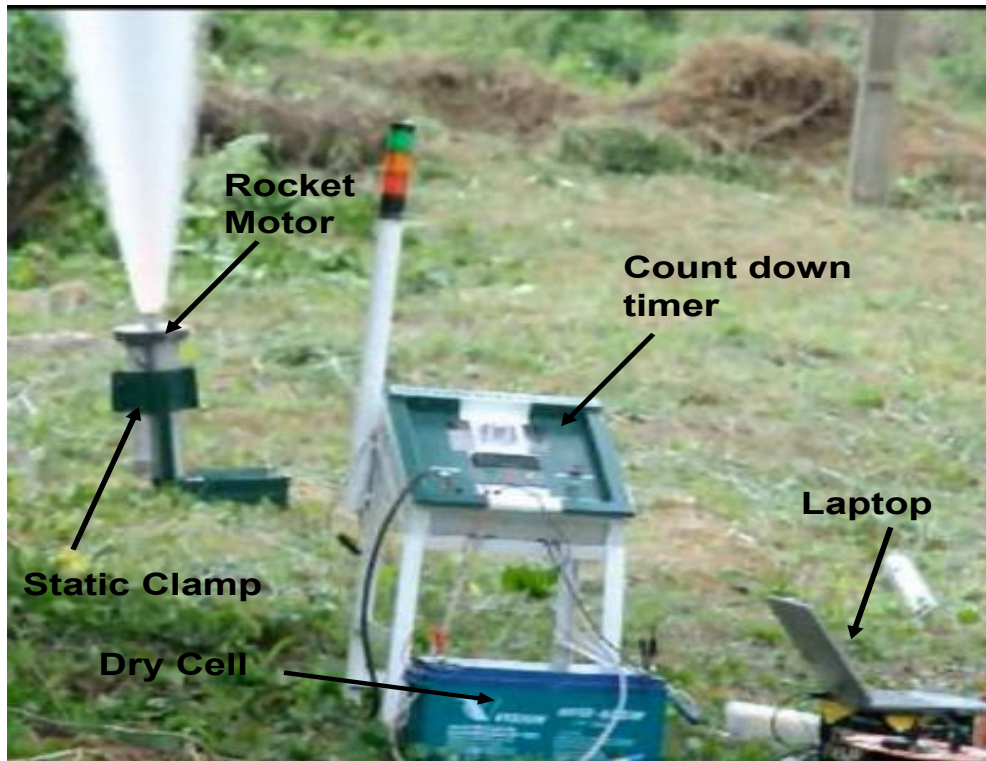


Fig. 9. Experimental setup for the static test

For a meaningful experiment, the following assumptions were made:

- I. It is possible that not all of the propellant was burned or that the motor case and nozzle were eroded by the high-velocity, high-temperature combustion gases. All the motors that were fired were weighed before, m_0 [kg], and after, m_f [kg], firing. It is assumed that not all of the propellant in the motor would be burnt after firing. The total amount of propellant ejected from the motor over the burn time, m_p [kg], was simply given by:

$$m_p = m_0 - m_f. \quad (19)$$

Thus, the propellant mass m_p is juxtaposed with the mass of the propellant before it was cased in the chamber to verify this assumption.

- II. Propellant would be ejected from the motors at a constant rate. An approximation of the propellant mass flow rate can be given by:

$$\dot{m} = \frac{m_p}{t_b}. \quad (20)$$

The motor burn time t_b is read-off from where the thrust data first increased continuously above the calibrated zero-thrust value-taken as t_1 . The motor burnout was taken to be where the thrust data first settled back down at the calibrated zero-thrust value minus m_p - taken as t_2 , hence $t_2-t_1=t_b$.

5. RESULTS AND COMPUTATIONS

In this section, the load cell readings are imported in to MATLAB where time versus thrust plots were made for each SRM. It is pertinent to note that the adopted specific impulse is 90s (average I_{sp} of SRM1-5), this formed the basis for computing our theoretical burn time and average thrust.

The thrust-time profiles of SRM 1-5 are depicted in Fig. 10.

In Table 3 below, t_{b1} and F_{avg1} represent the analytical computed values of burn time and average thrust from the mathematical expression in (10) and (16) respectively, while, t_{b2} and F_{avg2} are their experimental counterparts.

6. DISCUSSION OF RESULTS

With Fig. 3 in perspective, the primary objective of amateur rockets typically used as sounding rocket, is to have a very short boost phase then a long sustained phase, such propulsion system is called a *boost-sustain* system. From Fig. 10, none of the SRMs have a combination of such trend. Some rocket motors are designed to provide their total impulse near the beginning of the flight; the motor burns out and provides no more thrust and then the rocket glides to its target. These types are called *boost-glide* rockets [15]. From Fig. 10, SRM 1, SRM 2 and SRM 5 are typically of a *boost-glide* propulsion system-having a short duration to attain the maximum thrust and then thrust begins to decline. Combustion kink is noticed in the form of a sudden spiked-thrust with SRM 5 at two points (1.6 s and 2.4 s). Similar kink is also visible at about 1.8s with SRM 2. Propellant characteristics have strong effect on the susceptibility of SRMs to kinks; changes in the binder, particle-size distribution, ratio of oxidiser to fuel and burn-rate catalysts can all cause kinks, oftentimes in an unpredictable manner [16]. The phenomenon of kink may also occur when perturbations excite oscillation modes of the chamber cavity. Also, interaction with combustion, flow, particles,

nozzle, etc., may induce either an increase or a decrease of the phenomenon. When it increases, pressure increase may consequently be driven to an unacceptable level [17]. Such type of motor behaviour is not desirable and in most cases discarded. SRM 3 and SRM 4 exhibit a sustained phase of the propulsion system, without an evident boost phase.

The thrust-time profile with the longest sustained phase and highest average thrust will surely attain the highest altitude. With this understanding in mind we examine all motors to see which one performs the best. Bearing in mind that SRM 2 and SRM 5 exhibit combustion kinks, they are therefore discarded. Even though SRM 5 and SRM 2 attained the highest thrust values of 2400N and 1750N respectively, combustion kinks can induces unwanted moment during the flight of a real rocket and perhaps cause the rocket to go off a predefined waypoint. SRM 3 sustains an average thrust of 720N for about 2 seconds, while SRM 4 sustained an average thrust of 664N for about 2.4 seconds. SRM 1 however sustained an average thrust of 739 N for just 1.6 s.

Apart from having longer burn time with a high average thrust (especially at the sustained

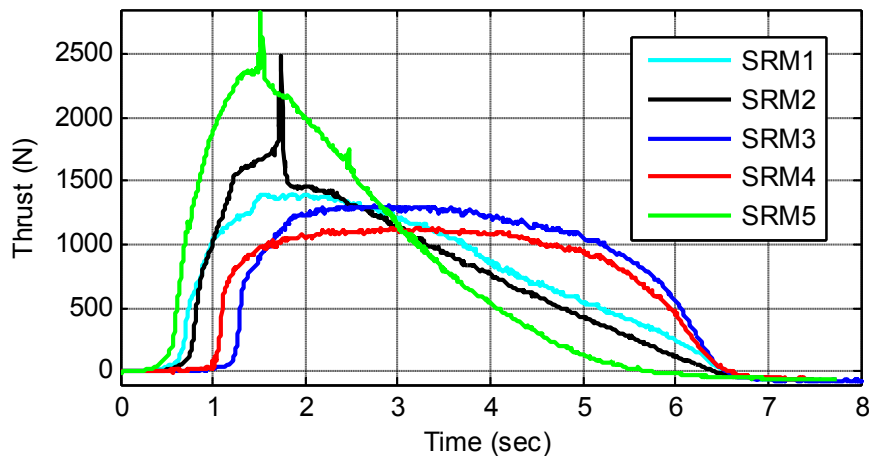


Fig. 10. Thrust-time trajectories of SMR1-SRM5

Table 3. Burn time and maximum thrust values of SRM1-5

| Motor | t_{b1} (s) | t_{b2} (s) | F_{avg1} (N) | F_{avg2} (N) | $t_{b1} - t_{b2}$ (s) | $ F_{avg1} - F_{avg2} $ (N) |
|-------|--------------|--------------|----------------|----------------|-----------------------|-----------------------------|
| SRM 1 | 7.96 | 7.3 | 709.6 | 739 | 0.66(8.3%) | 29.4(4.1%) |
| SRM 2 | 7.96 | 7.5 | 709.6 | 690 | 0.46(5.8%) | 19.6(2.8%) |
| SRM 3 | 7.96 | 7.6 | 709.6 | 720 | 0.36(4.5%) | 10.4(1.5%) |
| SRM 4 | 7.96 | 7.4 | 709.6 | 664 | 0.56(7%) | 45.6(6.4%) |
| SRM 5 | 7.96 | 7.8 | 709.6 | 708 | 0.16(2%) | 1.6(0.2) |

phase), one of the great advantages of testing a solid rocket motor before assembling it into a rocket, is the beauty of having an idea of the delay time before a particular rocket takes-off from the launch pad. From the thrust-time profile, thrust values up to the lift-off force of the rocket on the *thrust-axis* will correspond to a time value on the *time-axis* for the expected delay. As such, delay before rocket lift-off is just the time it takes for propulsion force build-up to overcome the weight of the rocket.

7. CONCLUSION

Mathematically derived formulation for burn time and average thrust as a function of propellant web thickness and motor length was put forward for SRM. The analytical values of burn time and average thrust for 5 motors (SRM1-5) were compared with experimental values obtained via DAQ system from a static bed test. Percentage errors of less than 10 per cent for each motor's burn time and average thrust were observed between experimental and analytical values. Thus, the novel mathematical expression for both the burn time and average thrust as a function of propellant web thickness and motor length gives a good correlation with experimental values.

Three motors meet the mission design of attaining a possible high altitude amongst the five motors investigated, though SRM 3 is expected to attain the highest altitude. This is deduced simply from the fact that since burn time translates to the time for powered flight, with a sustained phase maintained for longer time duration at a reasonably higher average thrust, a rocket with SRM 3 as motor will result in a higher altitude at the end of the rocket's flight (powered phase with coasting phase). Two motors SRM 2 and SRM 5 are advised to be discarded due to observed kinks in their thrust-time profile.

ACKNOWLEDGEMENT

We acknowledge the effort of all staff of Avionics, Rocket Fuel Development and Thrust Chamber Divisions at CSTP.

COMPETING INTERESTS

Authors have declared that no competing interests exist.

REFERENCES

- Zaehring AJ. Solid propellant rockets – an introductory handbook, American Rocket Co., Wyandotte, Michigan, USA; 1995.
- Sutton GP, Biblarz O. Rocket propulsion elements, 7th ed., John Wiley & Sons, Inc., New York. exnet, "Motor Test Stand," Google Search; 2001.
Available:<http://www.texnet.net/ccent/rockets/TestStand/TestStand.htm>
- Alian Davenas Solid rocket propulsion system. ISBN 0-08-040999-7; 1993.
- Estes Industries, 2006 Estes catalogue, Estes-Cox Corp., Penrose, USA, 2005.
- Stuart Leslie, James Yawn. Proposal for the inclusion of KNO₃/sugar propellants the TRA experimental rocketry program; 2002.
- Phung PV, Hardt AP. Burning rates of solid propellants by a variable pressure method. Explosive Stoffe. 1968;1(2):274-80.
- Kishore K, Sridhara K. Solid propellant chemistry. Defence Research & Development Organisation Ministry of Defence New Delhi-110 011. ISBN: 81-86514-02-6; 1999.
- ATK Space Propulsion Catalogue. Approved for public release. OSR No. 08-S-0259 and OSR No. 08-S-1556; Export Authority ITAR 125.4(b)(13); 2008.
- Miller WH, Barrington DK. A review of contemporary solid rocket motor performance prediction techniques. J. Space Roc. 1970;7(3),1970.
- Ajinkya V, et al. Decomposition of solid propellants in a combustion chamber. Advanced Chemical Engineering Research (ACER). 2012;1(1).
Available:www.seipub.org/acer
- Berko Zecevic, et al. Some design features of solid propellant rocket motors for shoulder-launched weapon systems. VIIIth International Armament Conference. Scientific Aspect of Armament & Safety Technology, Pultusk, Poland; 6-8.10. 2010.
- Patan Stalin, Santosh Kumar YNV, Nazumuddin SK. Design and geometrical analysis of propellant grain configurations of a solid rocket motor. IJEDR. 2014;2(4), ISSN: 2321-9939.
- Stephen A. Whitmore, Shannon D. Eilers. Leveraging Utah State's experimental rocketry program for a senior-design capstone course. 45th AIAA/ASME/SAE/ASEE Joint

- Propulsion Conference & Exhibit2 - Denver, Colorado, 5 August 2009.
14. Tse FS, Morse IE. Measurement and instrumentation in engineering – principles and basic laboratory experiments. Marcel Dekker, Inc., New York and Basel; 1989.
 15. Military Handbook, Missile flight simulation part one, Surface-To-Air Missiles, MIL-HDBK-1211(MI); 1995.
 16. Marc Faria Gomes. Internal ballistics simulation of a solid propellant rocket motor. Master's Degree Dissertation. Universidade da Beira Interiore Ngenharia; 2013.
 17. Alian Davenas. Solid rocket propulsion system. ISBN 0-08-040999-7; 1993.

© 2015 Aliyu et al.; This is an Open Access article distributed under the terms of the Creative Commons Attribution License (<http://creativecommons.org/licenses/by/4.0>), which permits unrestricted use, distribution, and reproduction in any medium, provided the original work is properly cited.

Peer-review history:
The peer review history for this paper can be accessed here:
<http://sciencedomain.org/review-history/10187>